ISSN 1063-7842, Technical Physics, 2014, Vol. 59, No. 5, pp. 629–636. © Pleiades Publishing, Ltd., 2014.
Original Russian Text © A.A. Koronovskii, O.I. Moskalenko, A.S. Pavlov, N.S. Frolov, A.E. Hramov, 2014, published in Zhurnal Tekhnicheskoi Fiziki, 2014, Vol. 84, No. 5, pp. 1–8.

THEORETICAL AND MATHEMATICAL PHYSICS

Generalized Synchronization in the Action of a Chaotic Signal on a Periodic System

A. A. Koronovskii, O. I. Moskalenko*, A. S. Pavlov, N. S. Frolov, and A. E. Hramov

Chernyshevsky State University, Astrakhanskaya ul. 83, Saratov, 410012 Russia
Gagarin State Technical University, Politekhnicheskaya ul. 77, Saratov, 410054 Russia
**e-mail: moskalenko@nonlin.sgu.ru*

Received October 3, 2012; in final form, August 9, 2013

Abstract—Generalized synchronization is observed during the action of a chaotic signal on generators of periodic oscillations. The features in the behavior of the synchronous regime threshold upon a change in the chaotic signal parameters are investigated. The possibility of using such devices for concealed information transfer is demonstrated.

DOI: 10.1134/S1063784214050132

INTRODUCTION

The study of synchronization of oscillations in coupled dynamic systems is an important trend in contemporary nonlinear dynamics [1]. The interest in this phenomenon is due to its fundamental importance [1] as well as the possibility of application of its various types in physiology, medicine, for concealed information transfer, and in other fields of science and engineering [2–4].

The regime of generalized synchronization (GS) is one of the most interesting types of random synchronization [5]. As a rule, it is considered for a system of two unidirectionally coupled stochastic oscillators (drive (master) oscillator $\mathbf{x(t)}$ and response (slave) oscillator $\mathbf{u(t)}$) and indicates the existence of the functional relation

$$\mathbf{u}(t) = \mathbf{F}[\mathbf{x}(t)] \quad (1)$$

between their states. In recent years, attempts have been made at generalizing this regime to mutually coupled systems and a network of coupled nonlinear elements [6–8]. However, analysis of this regime in systems with unidirectional coupling is still topical.

One of the aspects that has not been studied comprehensively is the possibility of GS stabilization in the case when the slave system is in a periodic regime. The characteristics of the interacting system must obviously affect the stabilization of synchronization substantially. However, the methods for diagnostics of the synchronous regime remain almost unchanged.

In this study, we analyze the location of the GS boundary on the plane "frequency of the chaotic signal—coupling parameter" for various values of the parameters of the slave system. As the objects of investigation, we choose both model systems (unidirectionally coupled Rössler oscillators [9]) and actual systems of beam-plasma origin (unidirectionally coupled low-voltage vircators [10]). It will be shown below that the threshold for the emergence of the synchronous regime changes abruptly[1] upon a change in the parameters of the external chaotic signal, which makes it possible to use such devices for concealed data transmission based on GS [3]. We propose a modification of this technique and consider its advantages over the original method.

1. GENERALIZED SYNCHRONIZATION REGIME AND METHODS OF ITS DIAGNOSTICS

Before describing our results, let us briefly consider the determination of the GS regime and the methods of its diagnostics in unidirectionally coupled systems. As mentioned in the Introduction, the synchronous regime in this case implies the establishment of functional relation (1) between the states of these systems. An analogous definition is applicable for the GS regime in the case of the interaction of a stochastic oscillator with a system exhibiting periodic dynamics.

For GS diagnostics in two unidirectionally coupled chaotic systems, the method of an auxiliary system [11] or the method for calculating conditional Lyapunov exponents [12] is traditionally used. Both methods can be used for analyzing GS in the case of action of a stochastic signal on a system with periodic dynamics. In this case, the implementation of these methods and the criteria for GS occurrence remain almost unchanged.

In accordance with the method of an auxiliary system, we consider, apart from slave system $\mathbf{u}(t)$, an

[1] A sharp variation of the synchronous regime threshold implies a considerable change in the threshold value of the coupling parameter corresponding to the stabilization of the GS regime for a weak variation of the control parameter.

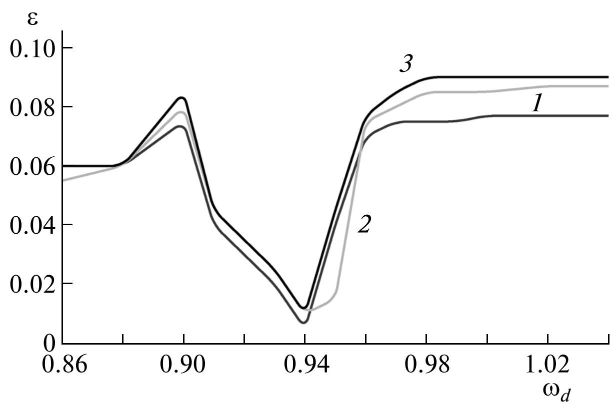

Fig. 1. Thresholds of the GS regime: $a = 0.08$ (*1*), 0.09 (*2*), and 0.094 (*3*) for two unidirectionally coupled Rössler oscillators (2) on the plane of parameters (ω_d, ε).

identical auxiliary $\mathbf{v}(t)$. The initial conditions for auxiliary system $\mathbf{v}(t_0)$ are chosen so that they differ from the initial conditions for slave system $\mathbf{u}(t_0)$, but lie in the attraction basin of the same attractor. In the absence of the GS regime between the interacting systems (naturally, if a periodic regime in the slave system differs from the limit cycle), the vectors of state $\mathbf{u}(t)$ and $\mathbf{v}(t)$ of the slave and auxiliary systems belong to the same attractor, but are different. In the GS regime, in view of the relations $\mathbf{u}(t) = \mathbf{F}[\mathbf{x}(t)]$ and, accordingly, $\mathbf{v}(t) = \mathbf{F}[\mathbf{x}(t)]$, the states of the slave and auxiliary systems must become identical after the completion of the transient process ($\mathbf{u}(t) \equiv \mathbf{v}(t)$), which is the criterion for the existence of GS between the master and slave oscillators.

In view of the unidirectional coupling between the systems, it is sufficient in the diagnostics of the GS regime by calculating the spectrum of Lyapunov indices to calculate these indices $\lambda_1^r \geq \ldots \geq \lambda_{N_r}^r$ for the slave system alone (so-called conditional Lyapunov indices). The criterion for the existence of GS in this case is a negative value of the higher conditional Lyapunov index λ_1^r, which is initially zero since the slave system is in the periodic regime. Clearly, in the case of weak detuning of the natural frequencies of the interacting systems, the GS regime is close to the phase locking regime [13].

Let us briefly consider the mechanisms for the emergence of GS in the case when a chaotic signal acts on a system exhibiting a periodic behavior. It was shown in [9] that during the interaction between two stochastic oscillators, irrespective of the type of their coupling (dissipative or nondissipative), the emergence of GS is determined by the balance between the suppression of intrinsic chaotic dynamics in the slave system and the excitation of stochastic oscillations in it under the action of the external signal from the master system. In the case under investigation, "intrinsic chaotic dynamics" is obviously absent in the slave system and, hence, the master system can easily impose its chaotic dynamics on it. In this case, the GS regime must appear for lower values of the coupling parameter as compared to the case of two coupled chaotic systems.

It would be interesting to analyze the behavior of the GS threshold upon a change in the parameters of the master system. In particular, it is known that the behavior of the GS threshold for two unidirectionally coupled stochastic oscillators on the plane "master system frequency–coupling parameter" substantially differs from the behavior of the thresholds of other known types of chaotic synchronization: in the range of considerable detuning of natural frequencies, the synchronous regime threshold is almost independent of the parameters of the master system, while in the range of weak detunings, the GS threshold sharply increases for some systems [14]. Let us consider the behavior of the GS threshold in the case of the interaction of a stochastic oscillator with a system exhibiting periodic behavior using some concrete examples. We begin with analysis of the model system.

2. GENERALIZED SYNCHRONIZATION IN MODEL SYSTEMS

As the first example, we consider two unidirectionally coupled Rössler systems. We choose the values of control parameters so that the master system exhibits chaotic dynamics and the slave system is characterized by periodic oscillations. This model is described in dimensionless form by the following system of differential equations:

$$\begin{aligned} \dot{x}_d &= -\omega_d y_d - z_d, \quad \dot{x}_r = -\omega_r y_r - z_r + \varepsilon(x_d - x_r), \\ \dot{y}_d &= \omega_d x_d + a_d y_d, \quad \dot{y}_r = \omega_r x_r + a_r y_r, \\ \dot{z}_d &= p + z_d(x_d - c), \quad \dot{z}_r = p + z_r(x_r - c), \end{aligned} \tag{2}$$

where $a_d = 0.15$, $p = 0.2$, and $c = 10$ are the control parameters and parameter ε characterizes the coupling between the oscillators. Control parameter $\omega_r = 0.95$ of the slave system, which characterizes the frequency of oscillations, was fixed, while analogous parameter ω_d of the master system was varied from 0.86 to 1.04 to set the detuning of the interacting oscillators. When the control parameter of the slave system is $a_r = 0.08$, a cycle of period 2 takes place in the system; analogously, a cycle of period 4 is observed for $a_r = 0.09$ and of period 8 for $a_r = 0.094$.

Figure 1 shows the position of the GS threshold of system (2) on the control parameters plane (ω_d, ε). Curves *1*, *2*, and *3* correspond to the GS threshold for $a_r = 0.08$, 0.09, and 0.094, respectively. The synchronous regime threshold was determined from the instant of transition of the zeroth Lyapunov exponent to the range of negative values and was then refined using the method of an auxiliary system. It can be seen from the figure that the simpler the regime taking place in the system, the lower the threshold value of the coupling parameter corresponding to the stabilization of the synchronous regime. Moreover, the thresholds of the synchronous regime in this case are much lower than analogous thresholds in the case of interaction of two coupled stochastic systems (cf. Fig. 1 and Fig. 1 from [14], which shows the GS threshold in system (2) with the same values of control parameters and $a_r = 0.15$); this confirms the theoretical argument considered in Section 1. At the same time, as in the case of two coupled stochastic systems, the GS threshold in all cases considered here in the range of strong detunings of the natural frequencies is almost independent of the parameter of the master system. However, an intense dip observed in the range of relatively low values of frequency detuning is not typical of systems exhibiting chaotic dynamics.

The emergence of this dip can be explained as follows. If the frequency of external stochastic force is close to the natural frequency of oscillations in the slave system, frequency sticking (and, hence phase locking) takes place. The slave system is in the periodic regime; therefore, the master system can easily impose its own chaotic dynamics on the slave system. In this case, the phase locking and GS thresholds approximately coincide, and the GS threshold demonstrates a "normal" behavior.[2] An analogous conclusion can be drawn proceeding from the theoretical considerations in Section 1. In the range of relatively low values of detuning, the phase locking regime is preceded by the transition of the conditional zeroth Lyapunov exponent to the region of negative values. Since this Lyapunov exponent is the highest for the slave system, the instant of its transition to the range of negative values corresponds to the GS threshold. Clearly, in the range of relatively low values of detuning of the frequencies of the coupled systems, these two thresholds must be very close to each other.

However, in the range of relatively high values of detuning of the natural frequencies, the emergence of GS is governed by another mechanism. As in the case of two coupled chaotic systems, the synchronous regime appears due to suppression of intrinsic dynamics of the slave system and excitation of random oscillations in it under the action of the master system.

At the same time, in spite of a qualitatively different behavior of the GS thresholds in the case of the interaction of two chaotic systems and a system demonstrating a periodic behavior and experiencing the action of a stochastic oscillator, the GS threshold changes very sharply in both cases upon a slight variation of the parameters of the external chaotic signal (in particular, upon a transition from the range of relatively high values of detuning to the range of relatively low values of detuning of the natural frequencies of the coupled systems, the critical value of the coupling parameter corresponding to the stabilization of the synchronous regime changes more than twofold), which makes it possible to use these systems for concealed information transfer [2, 15, 16].

3. GENERALIZED SYNCHRONIZATION IN SYSTEMS OF BEAM–PLASMA ORIGIN

As the second example, we consider the stabilization of the GS regime in systems of the electron–wave origin, viz., a chain of two unidirectionally coupled low-voltage vircators [17].

A low-voltage vircator is a planar diode gap pierced by an electron flow with a supercritical perveance [10]. The supercritical perveance is produced by applying a decelerating potential to the output grid of the system; upon an increase in this potential, a virtual cathode (potential barrier reflecting a part of electrons back to the plane of injection and modulating the transmitted flow) is formed in the electron flow.

To simulate nonlinear transient processes in the beam of charged particles with a virtual cathode, a 1D model of the drift gap with a decelerating field was used. The simulation was performed using the particle-in-cell method [18]. In accordance with this method, the electron flow was represented as an aggregate of coarse particles (charged sheaths) injected in equal time intervals with a constant velocity into the interaction space. For each coarse particle, the nonrelativistic equations of motion are solved, which can be written in dimensionless variables in the form

$$\frac{d^2x_i}{dt^2} = -E(x_i), \quad (3)$$

where x_i is the coordinate of the ith particle and $E(x_i)$ is the field of the space charge at the point with coordinate x_i.

The field strength and the potential of the space charge are determined on a uniform 3D mesh with a spacing Δx that covers the intermesh space. The space charge field potential in the quasi-static approximation is defined by the Poisson equation, which in the 1D approximation has the form

$$\frac{d^2\varphi}{dx^2} = \alpha^2\rho(x), \quad (4)$$

where $\alpha = \omega_p L/v_0$ is the Pierce parameter (ω_p is the plasma frequency, L is the length of the drift gap, and v_0 is the unperturbed velocity of the electron flow). The boundary condition to the Poisson equation is the condition imposed on the decelerating potential difference applied between the grids of the system: $\varphi(0) = 0$ and $\varphi(1) = \Delta\varphi$. Field E of the space charge in this case is determined by numerical differentiation of the resultant values of the potential.

[2] By "normal" behavior here we mean an increase in the threshold value of the coupling parameter corresponding to stabilization of the synchronous regime upon an increase in detuning between the systems.

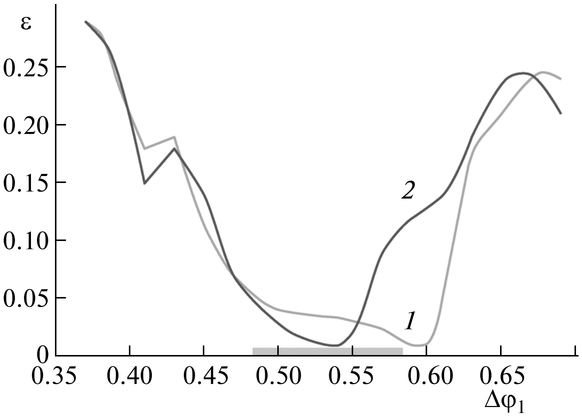

Fig. 2. GS thresholds in a system of two unidirectionally coupled low-voltage vircators on the plane of parameters ($\Delta\varphi_1$, ε) for $\Delta\varphi_2 = 0.6$ (complex-periodic regime, curve *1*) and $\Delta\varphi_2 = 0.525$ (chaotic regime, curve *2*).

The electron flux density is calculated by the particle-in-cell method, which involves the bilinear weighing of the charge of coarse particles on the mesh for determining the space charge [18]. In this method, the space charge density at the *j*th point of the 3D mesh ($x_j = j\Delta x$) is given by

$$\rho(x_j) = \frac{1}{n_0}\sum_{i=1}^{N}\Theta(x_i - x_j), \qquad (5)$$

where N is the total number of coarse particles, n_0 is the parameter of the computational algorithm, which is equal to the number of particles per cell in the unperturbed state, and

$$\Theta(x) = \begin{cases} 1 - |x|/\Delta x, & |x| < \Delta x \\ 0, & |x| > \Delta x \end{cases} \qquad (6)$$

is the piecewise linear function determining the weighing procedure for a coarse particle on the 3D mesh with spacing Δx.

To extract the power of microwave oscillations in the virtual cathode in the low-voltage vircator, the segment of the spiral slow-wave structure (SSWS) was used, which was simulated by the equivalent circuit method [19]. In accordance with this method, an SSWS segment is described by the telegraph equations supplemented with the term describing the excitation of electromagnetic waves by a beam:

$$\frac{\partial I}{\partial t} = -\frac{1}{L}\frac{\partial U_{\text{out}}}{\partial x}, \quad \frac{\partial U_{\text{out}}}{\partial t} = -\frac{1}{C}\frac{\partial I}{\partial x} + \frac{1}{C}\frac{\partial q}{\partial t}, \qquad (7)$$

where U_{out} is the output signal from the low-voltage vircator (integrated quantity characterizing the state of the system). The telegraph equations were solved numerically under the assumption of matching of the transmission line at the left ($x = 0$) and right ($x = l$) ends of the SSWS segment. The charge distribution $q(t, x)$ of the beam exciting electromagnetic waves in the transmission line was taken from the solution of the problem by the particle-in-cell method (see above).

To study the GS in a chain consisting of two unidirectionally coupled low-voltage vircators, we simulated numerically the dynamics of the master (with subscript 1) and slave (subscript 2) oscillators in accordance with the above equations (3)–(7). The unidirectional coupling between the low-voltage vircators was realized by applying a microwave signal from the output of the master oscillator to the input of the slave oscillator [17]. The signal was introduced into the beam in the slave oscillator by modulating the flow entering the diode gap by the segment of the spiral located between the electron gun and the input grid of the interaction space to which the output signal from the master vircator was supplied. The communication channel between the oscillators contained an attenuator that was used for controlling the power of the microwave signal acting on the slave oscillator. In the model under investigation, this was taken into account by supplementing the equations for the slave oscillator with additional equations describing the modulating spiral:

$$\frac{\partial I_{2\text{in}}}{\partial t} = -\frac{1}{L}\frac{\partial U_{2\text{in}}}{\partial x}, \quad \frac{\partial U_{2\text{in}}}{\partial t} = -\frac{1}{C}\frac{\partial I_{2\text{in}}}{\partial x}, \qquad (8)$$

with the boundary condition

$$U_{2\text{in}}(0, t) = \sqrt{\varepsilon}\, U_{1\text{out}}(1, t - T), \qquad (9)$$

where ε is the coupling coefficient in the system, which is introduced as the ratio of the power of the signal supplied to the modulator to the output power of the master oscillator.

The control parameters in the system of coupled low-voltage vircators are the decelerating potential difference $\Delta\varphi_{1,2}$ between the grids of the drift gap, beam current $\alpha_{1,2}$, and coupling coefficient ε. By varying the decelerating potential of the output grid and the Pierce parameter, it is possible to change the dynamics of the electron beam in the oscillator and the regime of oscillations in the virtual cathode.

As in the case of the model systems considered in Section 2, the master oscillator characterized by output signal $x(t) = U_{\text{out}1}(t)$ was tuned to the chaotic regime, while the slave oscillator characterized by output signal $u(t) = U_{\text{out}2}(t)$ was tuned to a complex-periodic regime. The values of the control parameters in this case were chosen as follows: decelerating potential $\Delta\varphi_2 = 0.6$ of the slave system and beam currents $\alpha_{1,2} = 0.9$ were fixed, and the decelerating potential of the master system was varied in the range $\Delta\varphi_1 \in [0.48; 0.58]$ ensuring chaotic oscillations in the system.

Figure 2 (curve *1*) shows the GS threshold in the plane "decelerating potential $\Delta\varphi_1$ of the master system–coupling parameter ε" for fixed values of all remaining control parameters. The same figure (curve *2*) shows the analogous threshold for $\Delta\varphi_2 = 0.525$ and for the same values of the remaining control parameters, which corresponds to realization of chaotic oscillations in the slave system. The synchronous regime threshold in both cases is determined using the auxiliary system method. Both thresholds are represented in a wider range of variation of parameter $\Delta\varphi_1 \in [0.37; 0.7]$, which corresponds to various regimes of oscillations in the master system (see [10] for details); the domain of chaos is shown by gray. It can be seen from the figure that the behavior of the GS threshold in this case is qualitatively analogous to that for model systems (see Fig. 1). The natural frequency of oscillations in the master system is close to the frequency of the slave oscillator in the entire range of variation of $\Delta\varphi_1 \in [0.48; 0.58]$; in view of the arguments given in Section 2, this indicates the closeness of the thresholds of the GS and phase locking regimes. In both cases, the threshold of occurrence of the synchronous regime changes sharply upon a slight variation of parameter $\Delta\varphi_1$; this makes it possible to use unidirectionally coupled low-voltage vircators for concealed information transfer based on GS [15]. This question will be considered in greater detail in the next section.

4. PRACTICAL APPLICATIONS OF GS

As mentioned above, concealed information transfer is one of the most important practical applications of the GS regime. Several methods of concealed information transfer based on this phenomenon have been developed (see, for example, [3, 16, 20–22, 25]), and the method developed in [22] and its modifications [15, 16] have the greatest advantages as compared to their analogs based in the GS regime as well as other types of synchronous behavior (phase locking and full synchronization; see review [3] for details). The main advantages of these methods are their high stability to noise and fluctuations in the communication channel and a simpler technical implementation, and the methods developed in [15, 16] are also characterized by a higher confidentiality in information transfer. At the same time, these methods have some drawbacks one of which is associated with instability of operation of these methods in the case when the parameters of the transmitting and receiving oscillators are not identical and cannot be eliminated completely. Like in the familiar analogs, these methods employ two identical stochastic oscillators, but in contrast to them, these oscillators are located on one side of the communication channel, which permits their adjustment.

The adjustment of the generators of chaotic oscillations is not always possible. Moreover, this problem is complicated during long-term operation of the devices, which renders the above methods inoperative in the long run. At the same time, as was established above in Sections 2 and 3, the GS regime can be observed not only in the case of action of a chaotic signal on stochastic generators, but also during the action of the same chaotic signal on generators of periodic oscillations. The development of identical generators

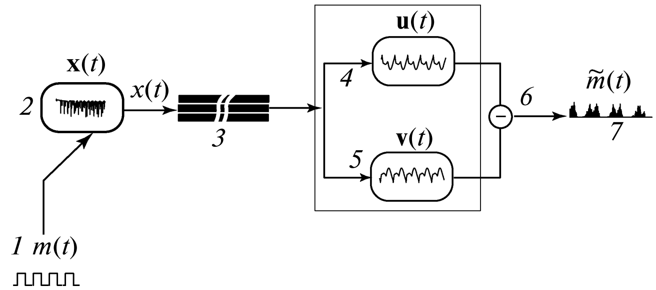

Fig. 3. Circuit diagram of concealed information transfer based on GS in the case of action of a chaotic signal on periodic oscillators: *1*—useful binary signal $m(t)$; *2*—first (transmitting) oscillator; *3*—communication channel; *4*—second (receiving) oscillator; *5*—third oscillator identical to second oscillator *4* as regards the control parameters; *6*—subtracter; and *7*—reconstructed useful signal $\tilde{m}$ (t).

of periodic oscillations is a less complicated problem than designing of chaotic oscillators. Moreover, the instability in the operation of oscillators with different parameters in the given case is manifested less strongly than in the case of chaos oscillators, which renders this scheme stable and operative for a long time. The quality of information transfer is higher in this case.

The circuit diagram for the implementation of the proposed method of information transfer is shown in Fig. 3. The concealed information transfer can be described as follows. Useful information signal $m(t)$ (*1*) is encoded in the form of a binary code. One or several control parameters of the transmitting (first) oscillator $\mathbf{x}(t)$ (*2*) is modulated by the information signal in such a way that the characteristics of the signal being transmitted change insignificantly, but the possibility of emergence/disappearance of the GS regime depending on the binary bit being transferred still exists. For implementing this feature, the GS threshold on the plane "modulation parameters–coupling strength" must have a singularity: upon a small change in the control parameter, the synchronous regime threshold must change sharply. The signal generated by the transmitting system is transferred along communication channel *3* in which it is affected by noise and distortions that are inevitably present in actual devices. The receiver is on the other side of the communication channel. It consists of two identical generators of periodic oscillations (second oscillator $\mathbf{u}(t)$ (*4*) and third oscillator $\mathbf{v}(t)$ (*5*)) that can be in the GS regime with transmitting oscillator *2*. The principle of operation of the receiver is based on the diagnostics of the GS regime with the help of the auxiliary system method. The signal from the communication channel is fed to the oscillators of the receiver. The signals at the output pass through subtracter *6* and then reconstructed useful signal *7* is detected, and this signal has the form of an alternating sequence of segments with asynchronous and synchronous behavior from which the initial information signal can easily be detected.

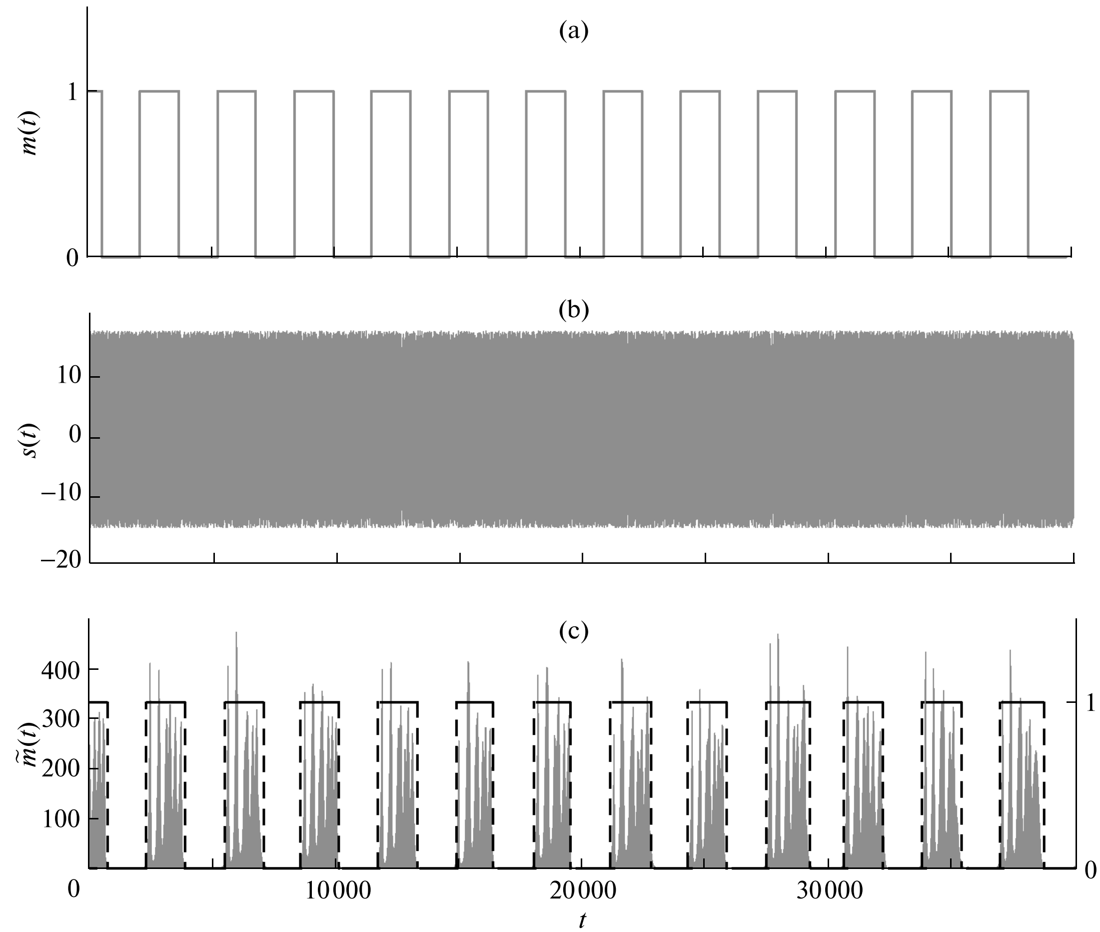

Fig. 4. Illustration of operability of the method for GS-based concealed information transfer in the case of Rössler systems used as the oscillators of the transmitting and receiving devices: (a) information signal $m(t)$ represented by a simple sequence 0/1 of binary bits; (b) $s(t)$ signal transmitted via the communication channel, and (c) reconstructed signal $\tilde{m}(t)$ (solid curve). The figure also shows the detected information signal (dashed line) after passing lower frequencies through the filter.

Let us illustrate the operability of the proposed method of information transfer using specific examples. As the oscillators of the transmitting and receiving devices, we choose the Rössler systems considered in Section 2 with the same values of control parameters a_d, p, c, and ω_r (low-voltage vircators considered in Section 3 with the same values of control parameters α and $\Delta\varphi_2$).[3] We will choose coupling parameter $\varepsilon = 0.06$ ($\varepsilon = 0.1$). For the modulation parameter, we choose the frequency ω_d of the master oscillator (decelerating potential difference $\Delta\varphi_1$); if binary bit 1 is transmitted during the preset time interval, we have $\omega_d = 0.95$ ($\Delta\varphi_1 = 0.52$) over this interval; if binary bit 0 is transmitted, parameter ω_d ($\Delta\varphi_1$) assumes the value 0.96 (0.54).

The operability of the proposed method of information transfer is illustrated in Fig. 4 (Fig. 5). Here, information signal $m(t)$ is represented by a simple sequence of binary bits 0/1 (Fig. 4a, 5a); signal $s(t)$ in the communication channel is the signal generated by transmitting chaos oscillator (Fig. 4b, 5b); reconstructed signal $\tilde{m}(t) = \mathbf{u}(t) - \mathbf{v}(t)^2$ before (solid line) and after (dashed line) the transmission through a low-frequency filter and the selection of threshold values (Fig. 4c, 5c). It can be seen from Figs. 4b and 5b that the modulation of control parameters in both cases does not noticeably change the characteristics of the signal produced by the transmitting chaos oscillator, which rules out the decoding of the information signal by a third party. At the same time, the quality of information reconstructed in the receiver is quite high. It can easily be seen that the signals shown in Figs. 4a and 5a (initial information signal) and the dashed line in Figs. 4c and 5c (detected information signal) coincide almost exactly, indicating the high quality of information transfer. An analogous situation is observed in the presence of noise in the communication channel, the ratio E_b/N_0 of the energy per bit to

[3] Here and below, we will indicate the values of parameters for the Rössler system and will give analogous values for low-voltage vircators in the parentheses.

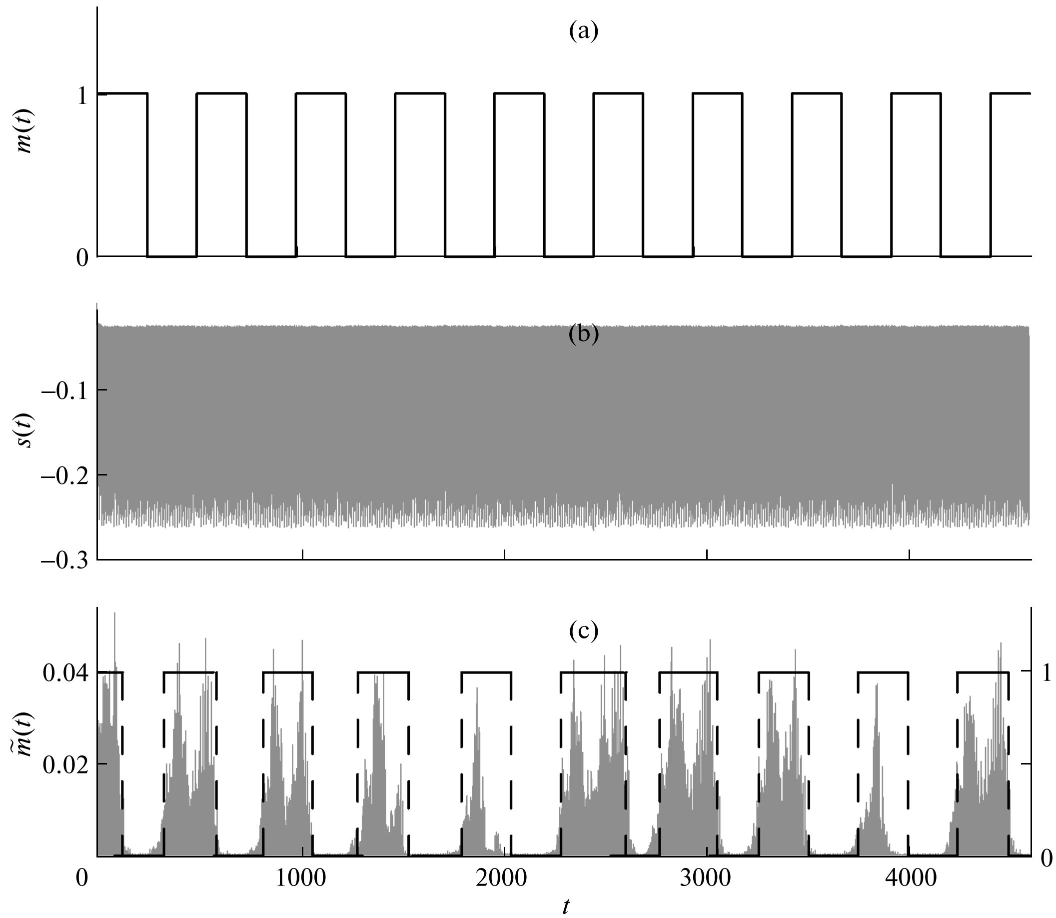

Fig. 5. Illustration of operability of the method for GS-based concealed information transfer in the case of low-voltage vircators used as the oscillators of the transmitting and receiving devices: (a) information signal $m(t)$ represented by a simple sequence 0/1 of binary bits; (b) $s(t)$ signal transmitted via the communication channel, and (c) reconstructed signal $\tilde{m}(t)$ (solid curve). The figure also shows the detected information signal (dashed line) after passing lower frequencies through the filter.

the spectral density of noise power [23] for which the method becomes inoperative being much lower (modulo higher) than in the case when chaos oscillators are used in the receiver.[4]

Thus, the method of information transfer proposed here solves the problem of instability of operation in the case when the parameters of the transmitting and receiving devices are not identical (moreover, these devices can be in basically different regimes of oscillations) and makes it possible to improve the noise stability and the quality of information transfer.

CONCLUSIONS

We have observed generalized synchronization during the action of a chaotic signal on a system in a periodic regime. It is shown for two different systems (unidirectionally coupled Rössler systems and low-voltage vircators) that the synchronous regime threshold is lower than for two coupled chaotic systems. We have analyzed the location of the GS threshold on the plane “detuning frequency–coupling strength” and explained the mechanisms of occurrence of the synchronous regime in the range of relatively high and relatively low values of detuning of natural frequencies. The possibility of using the observed regime for concealed information transfer has been demonstrated. It is found that the use of generators of periodic oscillations in the receiver solves the problem of instability of operation of the method in the case of different control parameters of the coupled systems and makes it possible to improve the noise stability and information transfer quality.

[4] It should be mentioned for comparison that the method of information transfer based on GS of chaotic oscillations with the Rössler systems as oscillators of the transmitter and receiver becomes inoperative when $E_b/N_0 = -10.01$ dB, while the method proposed here and using the same Rössler systems with control parameters of receiving oscillators corresponding to periodic oscillations with a period of 8 in them effectively operates up to $E_b/N_0 = -22.75$ dB.

ACKNOWLEDGMENTS

This study was supported by the Russian Foundation for Basic Research (project nos. 12-02-33071 and 14-02-31204) and the Grant Council of the President of the Russian Federation within the program supporting young Russian doctors of sciences (project MD-345.2013.2).

REFERENCES

1. A. Pikovsky, M. Rosenblum, and J. Kurths, *Synchronization: Universal Concept in Nonlinear Sciences* (Cambridge Univ., Cambridge, 2001).
2. O. V. Sosnovtseva, A. N. Pavlov, E. Mosekilde, K. P. Yip, N. H. Holstein-Rathlou, and D. J. Marsh, Am. J. Physiol. Renal. **293**, F1445 (2007).
3. A. A. Koronovskii, O. I. Moskalenko, and A. E. Khramov, Phys. Usp. **52**, 1213 (2009).
4. J. van Luijtelaar, A. E. Hramov, E. Yu. Sitnikova, and A. A. Koronovskii, J. Clin. Neurophysiol. **122**, 687 (2011).
5. N. F. Rulkov, M. M. Sushchik, L. S. Tsimring, and H. D. I. Abarbanel, Phys. Rev. E **51**, 980 (1995).
6. Z. Zheng, X. Wang, and M. C. Cross, Phys. Rev. E **65**, 056211 (2002).
7. S. Guan, X. Wang, X. Gong, K. Li, and C. H. Lai, Chaos **19**, 013130 (2009).
8. O. I. Moskalenko, A. A. Koronovsk, A. E. Hramov, and S. Boccaletti, Phys. Rev. E **86**, 036216 (2012).
9. A. A. Koronovskii, O. I. Moskalenko, and A. E. Khramov, Tech. Phys. **51**, 143 (2006).
10. Yu. A. Kalinin, A. A. Koronovskii, A. E. Khramov, E. N. Egorov, and R. A. Filatov, Plasma Phys. Rep. **31**, 938 (2005).
11. H. D. I. Abarbanel, N. F. Rulkov, and M. M. Sushchik, Phys. Rev. E **53**, 4528 (1996).
12. K. Pyragas, Phys. Rev. E **56**, 5183 (1997).
13. G. V. Osipov, B. Hu, C. S. Zhou, M. V. Ivanchenko, and J. Kuths, Phys. Rev. Lett. **91**, 024101 (2003).
14. A. E. Hramov, A. A. Koronovskii, and O. I. Moskalenko, Europhys. Lett. **72**, 901 (2005).
15. O. I. Moskalenko, A. A. Koronovskii, and A. E. Hramov, Phys. Lett. A **374**, 2925 (2010).
16. A. A. Koronovskii, O. I. Moskalenko, and A. E. Khramov, Tech. Phys. **55**, 435 (2010).
17. N. S. Frolov, A. A. Koronovskii, and A. E. Khramov, Izv. Ross. Akad. Nauk, Ser. Fiz. **75**, 1697 (2012).
18. C. K. Birdsall and A. B. Langdon, *Plasma Physics, via Computer Simulation* (McGraw-Hill, New York, 1985).
19. E. N. Egorov, Yu. A. Kalinin, A. A. Koronovskii, A. E. Khramov, and M. Yu. Morozov, Tech. Phys. Lett. **32**, 402 (2006).
20. J. Terry, and G. Van Wiggeren, Chaos, Solitons and Fractals **12**, 145 (2001)).
21. K. Murali and M. Lakshmanan, Phys. Lett. A **241**, 303 (1998).
22. A. A. Koronovskii, O. I. Moskalenko, P. V. Popov and A. E. Khramov, Izv. Ross. Akad. Nauk, Ser. Fiz. **72**, 143 (2008).
23. B. Sklar, *Digital Communications: Fundamentals and Applications* (Prentice-Hall, 2001).

Translated by N. Wadhwa